International Journal of Control, Automation, and Systems (2013) 11(6):1214-1222 ISSN:1598-6446 eISSN:2005-4092
DOI 10.1007/s12555-012-0076-3 http://www.springer.com/12555

Optimal Signal Tracking Algorithm for GNSS Signal using Moving Set-point LQG System

Sanghoon Jeon, Chongwon Kim, Ghangho Kim, Ojong Kim, and Changdon Kee*

Abstract: This paper proposes moving set-point state feedback for a LQG control system. In contrast to the independent code and carrier tracking loop of a conventional receiver algorithm, the code and carrier tracking variables are correlated in the LQG system. Not only are the multiple states correlated with each other, but also the control inputs are formulated from a combination of the states and the optimal LQG controller gain. In addition, this paper develops a moving set point to estimate the GNSS signal more accurately. To analyze the advantage of the proposed method, a signal tracking simulation using hardware GNSS simulator is performed and the simulation results show that the tracking performance of the moving set-point LQG system is better than that of a conventional loop filter, especially in terms of the code tracking performance.

Keywords: GNSS, LQG, optimal tracking, signal tracking, software defined radio.

1. INTRODUCTION

GNSS navigation signal tracking is different from conventional communication signal tracking [1]. Unlike that the maintenance of the signal receiving power is the most important to get better bit error rate in the conventional communication tracking, the signal tracking for navigation focuses on both the maintenance of the signal power and on the noise performance of the code and carrier phase for all visible satellites. Therefore many researcher studying GNSS signal tracking have tried to improve the code and carrier phase performance which is directly connected to positioning accuracy.

In this paper, the Kalman filter (KF) and a linear quadratic Gaussian (LQG) system [2] are implemented to improve the code and carrier tracking performance. In contrast to a conventional loop filter, which uses an independent code and a carrier tracking structure, the proposed system integrates the code and carrier tracking structure into multiple states. In the proposed system, the control inputs do not stem directly from states estimations but from a combination of the states and the optimal LQG controller gain.

Manuscript received February 14, 2012; revised May 21, 2013; accepted August 22, 2013. Recommended by Editorial Board member Duk-Sun Shim under the direction of Editor Myotaeg Lim.

This research was supported by a grant from "Development of Wide Area Differential GNSS," which is funded by the Ministry of Oceans and Fisheries of the Korean government, contracted through SNU-IAMD at Seoul National University.

Sanghoon Jeon, Chongwon Kim, Ghangho Kim, Ojong Kim, and Changdon Kee are with the School of Mechanical and Aerospace Engineering and the Institute of Advanced Aerospace Technology, Seoul National University, Gwanak 599 Gwanak-ro, Gwanak-gu, Seoul 151-742, Korea (e-mails: {dori8011, nan772, chew79, laywind0, kee}@snu.ac.kr).

* Corresponding author.

Several studies have investigated global navigation satellite system (GNSS) signal tracking loop using the KF. [3] demonstrated signal tracking using a smoother based on an extended KF (EKF). [4] used a two-state KF for carrier phase tracking. [5] categorized KF implementations using a state vector and measurements. In these researches, the control input generation scheme uses not the control gain but state feedback. Another study [6] developed a LQG controller for Galileo E1 signal tracking loop using an optimal regulation scheme.

In this paper, the implemented LQG system uses the discriminator outputs as the measurements input. Compared to the use of a conventional loop filter, there are two main advantages of the LQG controller system. The first of these is that the noise performance of the code tracking process increases due to aiding from the Doppler estimation. The second advantage is the expandability of the system. If there is some additional information from another sensor or position filter, the states are estimated more precisely. In a GNSS-inertial measurement unit (IMU) integrated system, for example, the Doppler frequency is estimated using a tightly coupled [7] or deeply coupled GNSS-IMU integration system [8]. Without an IMU, as another example, the expandability of integration of signal tracking and navigation filter such as vector tracking loop [9,10] can be increased if the LQG controller is adopted.

This paper proposes moving set-point state feedback with a LQG control system. Because the set points of proposed system are not certain values but time variables, the states are estimated at every epoch, and the set point moves along the estimated states. The concept of the proposed method is similar to the LQG controller for Galileo E1 signal tracking loop which is proposed in [2]. This paper, however, shows a unique tracking loop using the LQG controller. As a result, while cost function in [2] does not converge to zero but a local minimum, however, all states and control inputs in this paper

converge to zero and so does the cost function.

To analyze the advantages of the proposed method, simulation tests using GNSS signal obtained by hardware simulator were performed. The aim of the simulations is to show tracking performance of the proposed system for various user situation such as static movement or high dynamic environment. The simulation results show that the tracking performance of the moving set-point LQG system is better than the conventional loop filter, especially for the code tracking performance.

The remainder of this paper is organized as follows. Section 2 introduces four different tracking loops using the KF and LQG system. The four different tracking loops are classified as to whether or not the KF is utilized and the LQG controller is implemented. Section 3 presents the state and measurement modeling based on the tracking loop implementation of the software GNSS receiver. The moving set-point LQG system model is also proposed in this section. In Section 4, the simulation of the Doppler rate change is performed for a high-dynamics environment. The results of the simulation are verified using a hardware simulator data in Section 5. The paper finishes with conclusions and an outline of future work.

2. GNSS SIGNAL TRACKING

2.1. Conventional tracking loop

The GNSS signal tracking process is a process that estimates the navigation data bit transition, the code phase, and the carrier phase using the correlation results between the incoming signal though a RF antenna and replicas in the receiver. The conventional signal tracking process consists of two independent tracking loops: code tracking loop and carrier tracking loop [1]. Fig. 1 shows a simple block diagram of the signal tracking process. The structures of the code and carrier tracking are similar to each other.

In the conventional tracking loop, the discriminator brings out tracking error. The discriminators from the integrated in-phase and quadrature-phase correlation become the measurement input of the local channel loop filter. To reduce measurement noise, the classic local channel loop filter consists of a low-pass filter [11]. Based on the filtered output, the tracking process controls the code and carrier replica rate using numerical controlled oscillator (NCO).

For the measurement, we used the code discriminator known as the early minus late normalized power discriminator [12]. This is expressed as follows:

$$\Delta\tilde{\tau} = \frac{1}{2}\frac{(I_E^2+Q_E^2)-(I_L^2+Q_L^2)}{(I_E^2+Q_E^2)+(I_L^2+Q_L^2)}\cdot\frac{c}{f_{code}}, \quad (1)$$

f_{code} : The frequency of the code bit,
c : The speed of the light (meter/sec),
I_E, Q_E : The correlation sums of the early code replica and the in-phase and quadrature carriers,
I_L, Q_L : The correlation sums of the late code replica and the in-phase and quadrature carriers.

For carrier tracking, we used the frequency and the phase discriminators as the dot-cross product and the arc tangent discriminator [12].

$$\Delta\tilde{f}(k) = \frac{I_p(k)\cdot Q_p(k-1)+I_p(k-1)\cdot Q_p(k)}{t(k)-t(k-1)}\cdot\frac{c}{2\pi\lambda}, \quad (2)$$

$$\Delta\tilde{\phi}(k) = ATAN(\frac{I_P}{Q_p})\cdot\frac{c}{2\pi\lambda}, \quad (3)$$

$I_p(k), Q_p(k)$: The k-th epoch correlation sums of prompt code replica and in-phase and quadrature carriers,
$t(k)$: The receiver time at the k-th epoch,
λ : The carrier wave length (meter/cycle).

2.2. Signal tracking using the Kalman filter

The KF can be used to replace the conventional local channel loop filter. In this paper, the implementation methods are categorized as the measurement of the KF and the generation of the control input.

2.2.1 In phase and quadrature phase measurement based the KF estimation

In two earlier studies [3,13], the baseband correlation and integration sums that are the in phase and quadrature correlation results (point A in Fig. 2) are used as the measurements of the KF to estimate the states. Because the in-phase and quadrature-phase integration sums are nonlinear measurements, the EKF is used. The measurement vector is given by

$$Z_{k,I,Q} = [I_P \quad Q_P \quad I_E \quad Q_E \quad I_L \quad Q_L]^T. \quad (4)$$

The state vector in this paper consists of the code delay error, carrier phase error and the Doppler

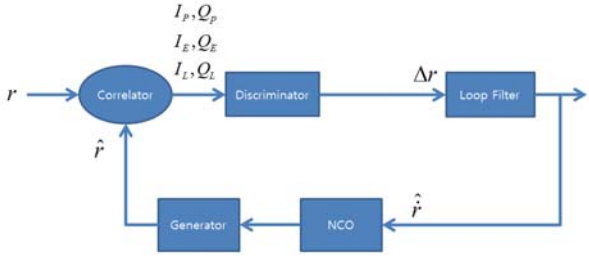

Fig. 1. A block diagram of the conventional GNSS signal tracking process.

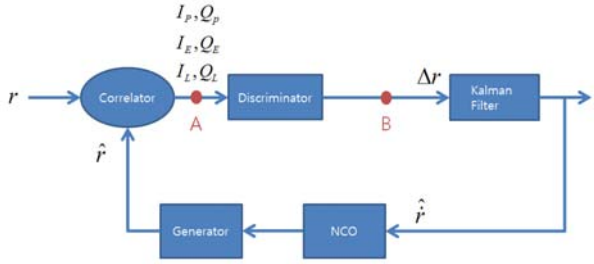

Fig. 2. The signal tracking loop using a Kalman filter.

frequency error which are given by

$$\delta X_{k,I,Q} = [\delta f_k \quad \delta\tau_k \quad \delta\varphi_k]^T. \tag{5}$$

2.2.2 Discriminator-based KF estimation

The discriminator-based KF uses the discriminator output (point B in Fig. 2) as the measurement input [5]. The measurement vector is given by

$$Z_{k,disc} = [\Delta\tilde{f} \quad \Delta\tilde{\tau} \quad \Delta\tilde{\varphi}]^T. \tag{6}$$

The state vector of the discriminator-based KF is similar to that in (5).

2.2.3 Discriminator based LQG tracking system

In another study [6], in contrast to the methods outlined in 2.2.1 and 2.2.2, which generate the NCO input using the estimated state error directly, the LQG tracking gain is implemented.

The earlier work [6] defined the state vector for the LQG tracking system as follows:

$$X_{k,LQG} = [\dot{\rho}_k \quad \delta\tau_k \quad \delta\varphi_k]^T. \tag{7}$$

Here, $\dot{\rho}_k$ is the Doppler frequency of the incoming signal of the k-th epoch. As in equation (6), the measurement vector of the LQG system is the discriminator output.

In the LQG system with the state vector (7) the Doppler frequency state converges to the Doppler frequency of the incoming signal. Therefore, not all states and control inputs converge to zero. The Doppler frequency in the state vector is not converged but is only estimated [6].

2.2.4 Moving set-point LQG tracking system

This paper proposes the moving set-point LQG tracking system. The measurement and state equations of the proposed system are similar to the LQG tracking system in 2.2.3. However, this system has a trim and de-trim process before and after the KF [14]. The nonlinear

Fig. 3. The signal tracking loop using the LQG regulation gain.

Fig. 4. The moving set-point signal tracking loop using LQG.

states and measurements are linearized at the trim points and the linearized system is recovered to the nonlinear system at de-trim points. This system makes the states and control input converge as rapidly as possible to the given set point. Because the Doppler and code/carrier phase keep changing with user and satellite movements during the GNSS tracking process, the estimated Doppler and code/carrier discriminator converge to the set point and the set point moves against the change of the signal variation versus time.

In most of linearization controller, there are some chances that there are many local minima. In the GNSS signal tracking problem, however, the initial states of control system is always in stable area because the signal acquisition process eliminates unstable control inputs, which are unstable input candidates of the initial states.

3. SYSTEM MODELING AND LQG CONTROLLER DESIGN

3.1. System modeling

When the signal tracking control is in a stable status, the relationship between the Doppler frequency and the estimated code rate and estimated carrier frequency is given by

$$\hat{\dot{\tau}}(t) = \dot{\rho}(t) + + n_c, \tag{8}$$

$$\hat{f}(t) = \dot{\rho}(t) + n_f, \tag{9}$$

where $\hat{\dot{\tau}}$ is the estimated code rate of the current tracking satellite, $\hat{f}$ is the estimated carrier frequency, n_c is the error of the estimated code rate and n_f is the error of the estimated carrier frequency.

Using (8) and (9), the continuous time states equation is given by

$$\begin{aligned}\dot{x} &= Fx + Gu + \overline{w} \\ &= \begin{bmatrix}0 & 0 & 0\\ 1 & 0 & 0\\ 1 & 0 & 0\end{bmatrix}\begin{bmatrix}\dot{\rho}\\ \Delta\tau\\ \Delta\varphi\end{bmatrix} + \begin{bmatrix}0 & 0\\ -1 & 0\\ 0 & -1\end{bmatrix}\begin{bmatrix}\hat{\dot{\tau}}\\ \hat{f}\end{bmatrix} + \begin{bmatrix}w_1\\ w_2\\ w_3\end{bmatrix},\end{aligned} \tag{10}$$

where w_1, w_2 and w_3 are the time-processing noises for each states. The discriminator-based measurement vector is identical to that of (6).

$$z = \begin{bmatrix}\Delta\tilde{f}\\ \Delta\tilde{\tau}\\ \Delta\tilde{\varphi}\end{bmatrix} \tag{11}$$

The relationship between the states and the measurements is given by [6]

$$\Delta\tilde{f} = \dot{\rho}_N - \hat{f} + \tilde{n}_f, \tag{12}$$

$$\Delta\tilde{\tau} = \Delta\tau_N + \tilde{n}_\tau, \tag{13}$$

$$\Delta\tilde{\varphi} = \Delta\varphi_N + \tilde{n}_\varphi. \tag{14}$$

Using (11)-(13), the measurement equation for the KF is given by

$$z = I_{3\times3}x + Du + v = \begin{bmatrix}1&0&0\\0&1&0\\0&0&1\end{bmatrix}x + \begin{bmatrix}0&-1\\0&0\\0&0\end{bmatrix}u + \begin{bmatrix}\tilde{n}_f\\\tilde{n}_\tau\\\tilde{n}_\varphi\end{bmatrix}, \quad (15)$$

where $\tilde{n}_f$ is the noise of the frequency discriminator, $\tilde{n}_\tau$ is the noise of the code discriminator and $\tilde{n}_\varphi$ is the noise of the phase discriminator.

To implement the software control loop, we convert (10) to the discrete form, as follows:

$$x_{k+1} = F_d x_k + G_d u_k + \bar{w}_k = \begin{bmatrix}1&0&0\\\Delta t&1&0\\\Delta t&0&1\end{bmatrix}x_k + \begin{bmatrix}0&0\\-\Delta t&0\\0&-\Delta t\end{bmatrix}u_k + \begin{bmatrix}w_{1,k}\\w_{2,k}\\w_{3,k}\end{bmatrix}. \quad (16)$$

3.2. Design of the moving set point with the LQG controller

This paper proposes that a LQG control system is added to the signal tracking system using KF estimation. In addition, a nonzero equilibrium state and the input of the LQG system are used. In other words, we create not states with the control input converge near zero but make them converge as rapidly as possible to equilibrium nominal set point values. The KF estimates, therefore, the state vector and control input using the trim results of the states and the measurement of the moving set point. The estimated state and control input values are then used in the de-trim process. From the de-trim process, the control input is generated for the next epoch. The set points of the states, measurements and control input are updated every epoch.

The state and control input trim processes are given by

$$\tilde{x}_k = x_k - x_k^* = \begin{bmatrix}\dot{\rho}_k\\\Delta\tau_k\\\Delta\varphi_k\end{bmatrix} - \begin{bmatrix}\dot{\rho}_k^*\\\Delta\tau_k^*\\\Delta\varphi_k^*\end{bmatrix}, \quad (17)$$

$$\tilde{u}_k = u_k - u_k^* = \begin{bmatrix}\hat{\tau}_k\\\hat{f}_k\end{bmatrix} - \begin{bmatrix}\hat{\tau}_k^*\\\hat{f}_k^*\end{bmatrix}, \quad (18)$$

$$\tilde{z}_k = z_k - z_k^* = z_k - \left(I_{3\times3}x_k^* + Du_k^*\right). \quad (19)$$

At the set point, the states equation of the result of the trim process is given by

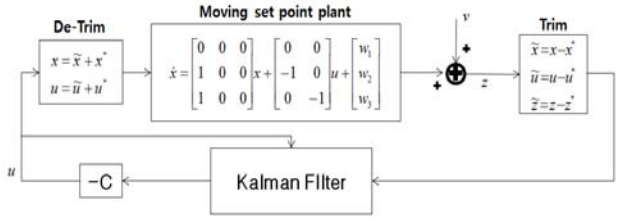

Fig. 5. A block diagram of the moving set-point Signal Tracking loop using LQG controller.

$$\tilde{x}_{k+1} = \begin{bmatrix}1&0&0\\\Delta t&1&0\\\Delta t&0&1\end{bmatrix}\tilde{x}_k + \begin{bmatrix}0&0\\-\Delta t&0\\0&-\Delta t\end{bmatrix}\tilde{u}_k + w_d. \quad (20)$$

The measurements equation is given by

$$\tilde{z}_k = I_{3\times3}\cdot\tilde{x}_k + D\tilde{u}_k + v_d, \quad (21)$$

where the processing noise and measurement noise are given by

$$w_d \sim N(0, Q_d),\ Q_d = diag(q_1, q_2, q_3),\quad v_d \sim N(0, R_d),\ R_d = diag(r_1, r_2, r_3). \quad (22)$$

Based on the signal models, we calculated LQG control gain using the cost function, which is given by

$$\min_{u_k} J = \min_{u_k} E\left[\sum_{k=1}^{N}(\tilde{x}_k^T A\tilde{x}_k + \tilde{u}_k^T B\tilde{u}_k)\right]. \quad (23)$$

The weighting matrices of the cost function are determined as follows:

$$A = \begin{bmatrix}\frac{1}{(\Delta\dot{\rho}_{\max})^2}&0&0\\0&\frac{1}{(\Delta\tau_{\max})^2}&0\\0&0&\frac{1}{(\Delta\varphi_{\max})^2}\end{bmatrix}, \quad (24)$$

$$B = \begin{bmatrix}\frac{1}{(\hat{\tau}_{\max})^2}&0\\0&\frac{1}{(\hat{f}_{\max})^2}\end{bmatrix}. \quad (25)$$

Here, $\Delta\dot{\rho}_{\max}$ is the maximum acceptable value of the Doppler value, $\Delta\tau_{\max}$ is the maximum acceptable value of the code phase discriminator, $\Delta\varphi_{\max}$ is the maximum acceptable value of the carrier phase discriminator, $\hat{\tau}_{\max}$ is the maximum acceptable increment value of the code NCO and $\hat{f}_{\max}$ is the maximum acceptable increment value of the carrier NCO.

4. SIMULATION RESULTS

4.1. Simulation environment

We performed the signal tracking simulation using a conventional loop filter and the moving set-point LQG system. Digitized RF baseband sample data were used. The simulation signal from a Spirent STR4500 hardware [15] simulator was collected using a NI PXIe5663 signal analyzer [16]. The intermediate frequency was zero, the sampling frequency was 12.5MHz, and the bandwidth was 25MHz. The quantization for ADC was 16bit I, Q data. The user movement is assumed to be in the static mode on the ground, and the C/N0 is about 41dB-Hz when the integration time is 1ms. The simulation was performed using MATLAB software GNSS receiver made by SNUGL [17].

To implement the LQG system with the simulation data, it was necessary to determine several design parameters that were the components of the processing noise matrix and the measurement noise matrix for the KF as well as the components of the weighting matrix to calculate the linear quadratic regulator (LQR) control gain.

For the KF implementation, the components of R_d are measured after an analysis of the measurement noise when the conventional loop filter is converged.

$$\begin{aligned}\sigma_{\Delta f} &= 24\,\text{Hz} \approx 5\,\text{m/s},\\ \sigma_{\Delta\tau} &= 0.03\,\text{chip} \approx 9\,\text{m},\\ \sigma_{\Delta\varphi} &= 0.1\,\text{rad} \approx 6\times10^{-2}\,\text{m}.\end{aligned} \tag{26}$$

The processing noise Q_d is determined by estimating the maximum change rate of the states.

$$\begin{aligned}q_{\dot\rho} &= \Delta\ddot\rho_{\max} = 0.15\,\text{m/s}^2,\\ q_{\tau} &= \Delta\dot\tau_{\max} = 0.01\,\text{chip/1ms} \approx 3\times10\,\text{m/s},\\ q_{\varphi} &= \Delta\dot\varphi_{\max} = 0.15\,\text{rad/1ms} \approx 1\,\text{m/s}.\end{aligned} \tag{27}$$

The components of the weighting matrices to calculate the LQR control gain are determined by Bryson's rule [18].

$$\begin{aligned}\Delta\dot\rho_{\max} &= 0.3\,\text{m/s},\\ \Delta\tau_{\max} &= 0.003\,\text{chip} = 1\,\text{m},\\ \Delta\varphi_{\max} &= 0.03\,\text{rad} = 2\times10^{-3}\,\text{m},\\ \Delta\hat{\dot\tau}_{\max} &= 0.017\,\text{chip/s} \approx 5\,\text{m/s},\\ \Delta\hat{\dot f}_{\max} &= 0.1\,\text{Hz} \approx 0.02\,\text{m/s}.\end{aligned} \tag{28}$$

For a stable system, the poles of the system matrix should be inside the unit disc [6]. However, the states equation, (15), is not controllable. Therefore, we modified the state equation slightly, as shown below.

$$\begin{aligned}\tilde x_{k+1} &= F_d'\tilde x_k + G_d'\tilde u_k + w_d\\ &= \begin{bmatrix}1-\varepsilon & 0 & 0\\ \Delta t & 1-\varepsilon & 0\\ \Delta t & 0 & 1-\varepsilon\end{bmatrix}\tilde x_k + \begin{bmatrix}0 & -\varepsilon\\ -\Delta t & 0\\ 0 & -\Delta t\end{bmatrix}\tilde u_k + w_d.\end{aligned} \tag{29}$$

We determined that ε is less than 10^{-4}. During the tuning process of ε, it is found that the larger value of ε might change the characteristics of the state transition. From (23) to (29), the LQG controller gain C was calculated using the DLQR function in the MATLAB toolbox [19].

$$\left[C, S, E\right] = DLQR\left(F_d', G_d', A, B\right). \tag{30}$$

Here, S is the Riccati equation solution and E is the closed-loop eigenvalues.

4.2. Simulation results

Fig. 6 shows the state estimation after the implementation of trim process in the moving set-point LQG system. It was noted that all of the states converge to zero with

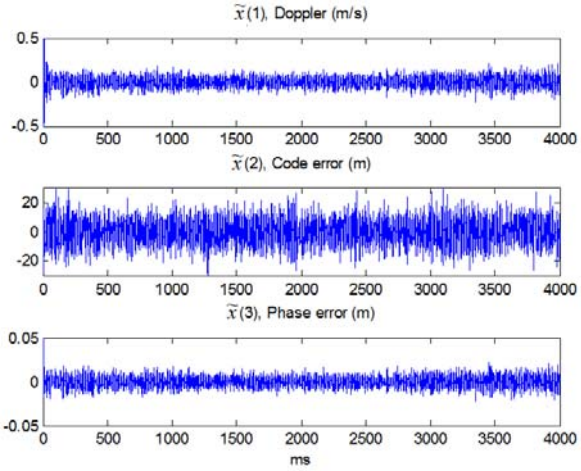

Fig. 6. Trim state estimation using the LQG controller.

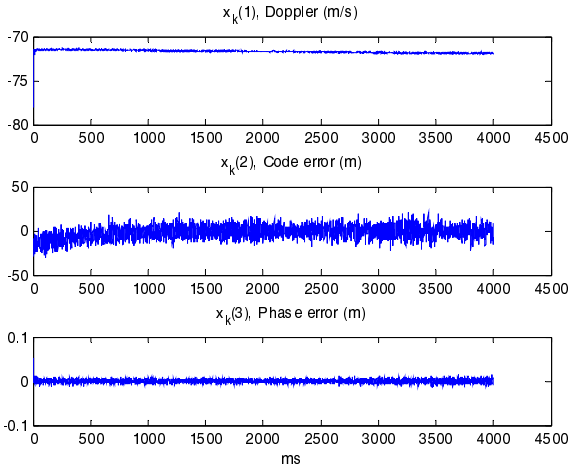

Fig. 7. The set-point variation using the LQG controller.

tracking jitter. In Fig. 7, the non-zero set-point states are shown. The Doppler frequency of the states converges to the incoming Doppler frequency as the KF converges.

To evaluate the tracking performance of the LQG system, we compared the proposed system to the conventional loop filter, which is implemented as the second loop low pass filter. The DLL bandwidths were 5 Hz and 1Hz for the comparison between the settling time and the steady states error. On the other hand, the PLL for carrier lock loop only uses 1 Hz bandwidth.

The simulation result of the code tracking loop is shown in Figs. 8 and 9. In steady state, the measurement noise performances of the conventional loop filter and the LQG controller are similar. For the variation of the control input, however, the code NCO noise level of the LQG controller is smaller than that of the conventional loop filter. Contrary to the independent code/carrier conventional loop filter, the states of the LQG controller are correlated with the estimated Doppler rate. Therefore, carrier tracking with relatively low noise measurements helps the code tracking loop track more precisely.

Figs. 10 and 11 show the simulation results of the carrier tracking loop. In this simulation, the conventional carrier tracking loop consists of FLL and PLL. To starts

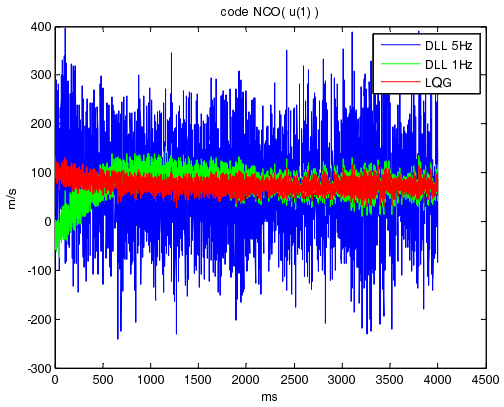

Fig. 8. The code NCO result (DLL vs. LQG system).

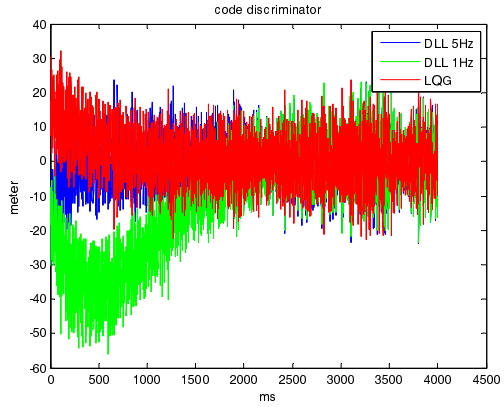

Fig. 9. The code discriminator measurements (DLL vs. LQG system).

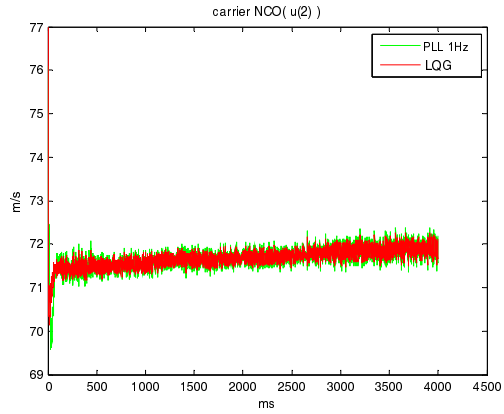

Fig. 10. The carrier NCO input (FLL/PLL vs. LQG controller).

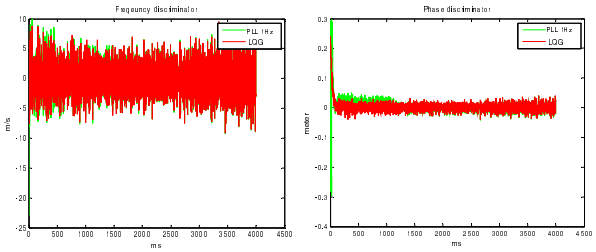

Fig. 11. The frequency and phase discriminator measurements (FLL/PLL vs. LQG system).

from 1 sec FLL runs for initial carrier tracking and then PLL runs for the normal carrier tracking process. The bandwidth of PLL is 1 Hz and FLL is 5 Hz.

The carrier tracking result also shows that the carrier NCO input noise level of the LQG controller is reduced compared to that of the conventional FLL/PLL. The frequency and phase discriminators of each tracking loop show similar results.

5. THE DOPPLER RATE CONSIDERATION

In Sections 3 and 4, we assume that the Doppler frequency is constant as the time varies. In the real world, however, the Doppler value changes according to the dynamics of the user and the GNSS satellites. Although the user may be in a static mode, the Doppler value changes due to the motion of the GNSS satellites and the rotation of the earth [12]. If we assume that the Doppler rate is constant, the Doppler time propagation can be shown as follows:

$$\dot{\rho}^j(k+1) = \dot{\rho}^j(k) + \ddot{\rho}^j(k)\Delta t + w_{k,0}. \tag{31}$$

Using (31), (20) is modified as follows:

$$x_{k+1} = \begin{bmatrix} 1 & 0 & 0 & 0 \\ \Delta t & 1 & 0 & 0 \\ 0 & \Delta t & 1 & 0 \\ 0 & \Delta t & 0 & 1 \end{bmatrix} x_k + \begin{bmatrix} 0 & 0 \\ 0 & 0 \\ \Delta t & 0 \\ 0 & \Delta t \end{bmatrix} u_k + \begin{bmatrix} w_{k,0} \\ w_{k,1} \\ w_{k,2} \\ w_{k,3} \end{bmatrix}. \tag{32}$$

The simulation results for the four-state equation are shown in Fig. 12 through Fig. 15. The simulation environment is identical to the data in Section 4.

Table 1 shows that the tracking performance of the proposed LQG system is better than that of the conventional loop filters. Though the settling time of the proposed system is longer than DLL 5 Hz case, in the steady-state error, the result of the proposed system outperforms the conventional loop filters.

The simulation result of the four-state equation is similar to that of the three-state equation because the Doppler rate of the incoming signal is not large enough to cause a difference in the tracking performance.

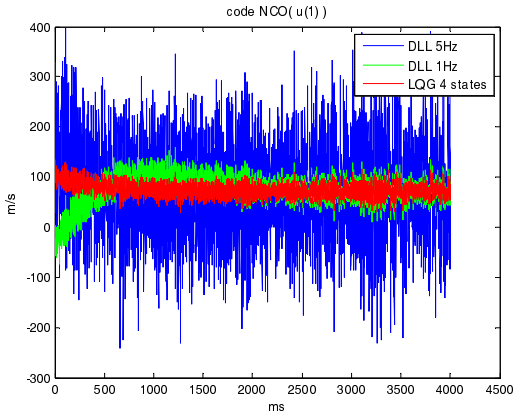

Fig. 12. The code NCO result (DLL vs. four-state LQG system).

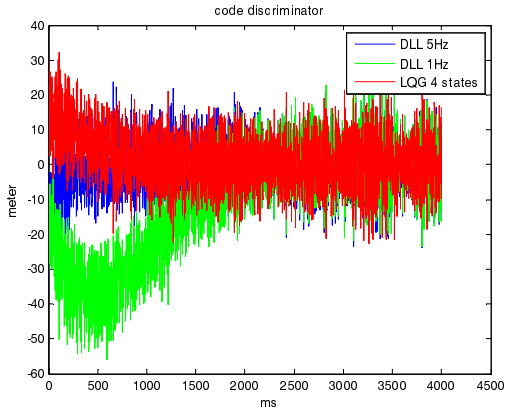

Fig. 13. The code discriminator measurements (DLL vs. LQG system).

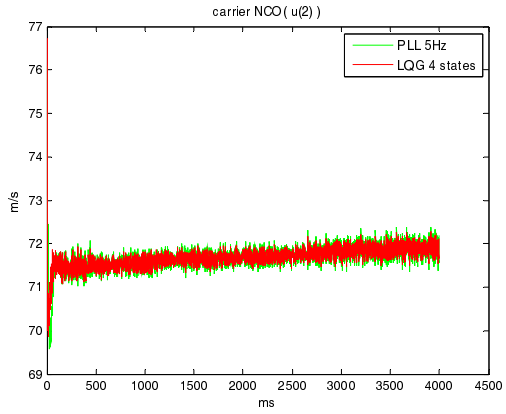

Fig. 14. The carrier NCO input (FLL/PLL vs. LQG controller).

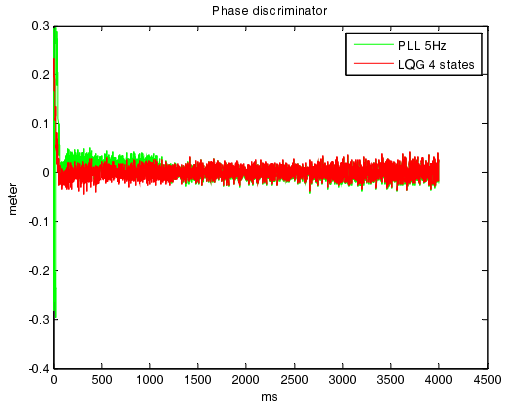

Fig. 15. Phase discriminator measurements (FLL/PLL vs. LQG system).

Table 1. Performance comparison of the conventional and proposed system.

	Steady-state standard dev.	Settling time
DLL 5Hz	251 m/s	700 ms
DLL 1Hz	24.0 m/s	2100 ms
LQG (proposed)	21.5 m/s	1100 ms

However, when the Doppler changes rapidly, such as in a low-earth-orbit (LEO) environment, or when the clock drift changes a lot due to the use of a low-cost TCXO in the GNSS receiver, the tracking performance of the LQG system can change.

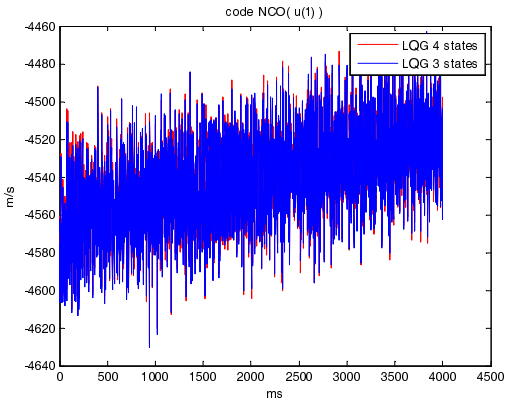

Fig. 16. The code NCO result (three-state vs. four-state LQG system).

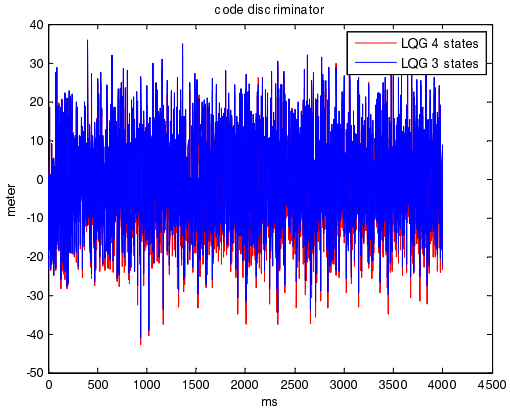

Fig. 17. The code discriminator measurements (three-state vs. four-state LQG system).

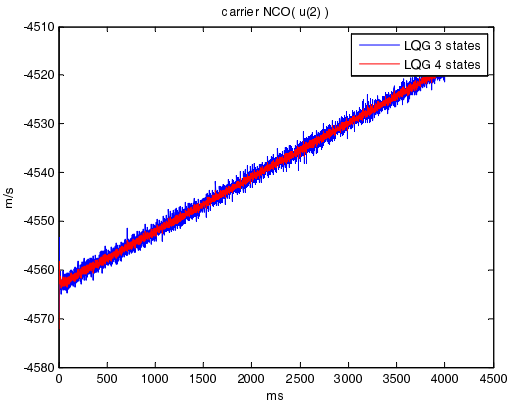

Fig. 18. The carrier NCO input (three-state vs. four-state LQG system).

To analyze the difference in each tracking performance, we tested the signal tracking process in a LEO environment simulation. The simulation signal was generated by a hardware simulator and the digitized baseband data was collected using a NI analyzer. The simulation results are shown in Fig. 16 through Fig. 19.

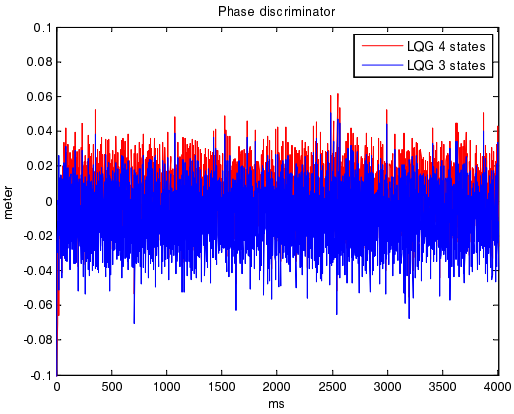

Fig. 19. Phase discriminator measurements (three-state vs. four-state LQG system).

For the code tracking results, the difference between each tracking performance was only slight. For the carrier tracking results, however, we noted a difference between the two LQG controllers. Fig. 18 shows the tracking performance of the carrier NCO as it affects the measurement noise during the navigation process. The four-state LQG controller tracks the incoming signal in a less noisy manner compared to the three-state LQG controller. In addition, the result of the three-state controller is slightly biased compared to that of the four-state controller, as shown in Fig. 19. Both the noise error and bias are directly related to the accuracy of the measurements for navigation.

To analyze the differences between two controllers, we defined the root mean square error (RMSE) value for the moving window. This is given by

$$\hat{\varphi}_k = \sqrt{\frac{\sum_{n=-m-1}^{m} \tilde{\varphi}_n^{\,2}}{2m}}. \tag{33}$$

Using (33), the RMSE values for the simulation results are shown in Fig. 20. The four-state LQG controller clearly shows better performance for a highly dynamic user.

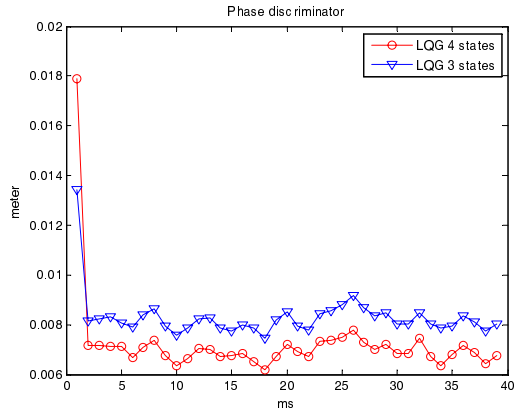

Fig. 20. RMSE of phase discriminator (three-state vs. four-state LQG system).

6. CONCLUSIONS

In this paper, we implemented a moving set-point LQG system for GNSS signal tracking. There are two advantages of the LQG controller as compared to the conventional loop filter. The first of these is the tracking performance. The simulation results show that the performance of the proposed LQG controller is superior in terms of the tracking noise performance to the conventional loop filter. The second advantage is the expandability of the proposed system. Contrary to the low-pass filtering of the conventional loop filter, the KF estimates the Doppler frequency and the Doppler frequency assists the code and carrier states. As the Doppler frequency is estimated more precisely, the tracking performance is improved. If we have additional information about the signal Doppler frequency and the user clock error from outside of the tracking process, the estimation may become even more accurate.

We implemented two types of state equations for the proposed LQG system. For a static user, the performance difference between each state equation is negligible. However, when the user moves very dynamically or when the reference clock in the receiver front-end is a very-low-cost TCXO, a different result can be expected from a larger matrix. In Section 5, the simulation result for the LEO scenario showed the differences in the tracking performance. The four-state KF, however, incurs an additional computation load from the heavy matrix calculation. As a result, we recommend three states to implement the LQG controller, except in the event of a high level of user dynamics or an environment with low-cost TCXO which may give rise to a severe clock-drift variation.

For future works, an integration of the LQG tracking system with user dynamics is one of good research theme, because the constitution of LQG system should be different for maximizing tracking performance. In addition, it is needed to study tracking loop which can enhance performance of the Doppler measurement. The simulation result of the proposed LQG system shows improved performance for code tracking but not carrier tracking. However there are many application which need high accurate Doppler such as attitude determination using the Doppler [20]. If the performance of the Doppler measurement increases due to the LQG system, its usefulness will be greatly upgraded.

REFERENCES

[1] A. J. V. Dierendonck, *Chap 8. GPS Receiver in Global Positioning System: Theory and Applications*, vol. 1, AIAA, Washington, 1996.

[2] B. D. O. Anderson and J. B. Moore, *Optimal Control, Linear Quadratic Methods*, Prentice-Hall International, Inc., Canberra, 1989.

[3] M. L. Psiaki, "Smoother-based GPS signal tracking in a software receiver," *Proc. of GPS ION*, pp. 2900-2913, 2001.

[4] K. H. Kim, G. I. Jee, and S. H. Im, "Adaptive vector-tracking loop for low-quality GPS signals," *In-*

ternational Journal of Control, Automation, and Systems, vol. 9, no. 4, pp. 709-715, December 2011.
[5] J. H. Won, D. Dotterbock, and B. Eissfeller, "Performance comparison of different forms of Kalman filter approach for a vector-based GNSS signal tracking loop," *Proc. of Institute of Navigation (ION GNSS 2009)*, pp. 3037-3048, 2009.
[6] G.-I. Jee, S.-H. Im, and B.-H. Lee, "Optimal code and carrier tracking loop design of Galileo BOC(1,1)," *Proc. of Institute of Navigation GNSS 2007*, pp. 2007.
[7] D. T. Knight, A. W. Osborne, R. W. Snow, and et al., "Demonstration of a new, tightly-coupled GPS/INS," *Proc. of the 6th ION GPS*, pp. 205-214, 1993.
[8] M. G. Petovello, D. Sun, and G. Lachapelle, "Performance analysis of an ultra-tightly integrated GPS and reduced IMU system," *Proc. of ION GNSS*, pp. 602-609, 2007.
[9] S. Kiesel, C. Ascher, D. Gramm, and G. F. Trommer, "GNSS receiver with vector based FLL-assisted PLL carrier tracking loop," *Proc. of ION GNSS 2008*, pp. 197-203, 2008.
[10] H. M. So, T. J. Lee, S. H. Jeon, C. W. Kim, C. D. Kee, T. H. Kim, and S. U. Lee, "Implementation of a vector-based tracking loop receiver in a pseudolite navigation system," *Sensors*, vol. 10, no. 7, pp. 6324-6346, 2010.
[11] J. B.-Y. Tsui, *Fundamentals of Global Positioning System Receivers - A Software Approach*, 2nd edition, John Wiley & Sons Inc., Texas, 2005.
[12] E. D. Kaplan, *Understanding GPS: Principles and Applications*, 2nd edition, Artech House, 2005.
[13] D. J. Jwo, "Optimisation and sensitivity analysis of GPS receiver tracking loops in dynamic environments," *IEE Proceeding of Radar, Sonar and Navigation*, vol. 148, no. 4, pp. 241-249, August 2001.
[14] A. E. Bryson, *Control of Spacecraft and Aircraft*, Princeton University Press, Princeton, 1994.
[15] STR4500 *GPS/SBAS Simulator with SimPLEX Software User Manual*, Spirent Communication Limited, 2002.
[16] NI PXIe-5663 Specifications.
[17] G. H. Kim, H. M. So, S. H. Jeon, C. D. Kee, Y. S. Cho, and W. S. Choi, "Development of modularized post processing GPS software receiving platform," *Proc. of International Conference on Control, Automation and Systems*, pp. 121-128, 2008.
[18] G. F. Franklin, J. D. Powell, and A. Emami-Naeini, *Feedback Control of Dynamic Systems*, 4th edition, Prentice Hall, Upper Saddle Receiver, NJ, 2002.
[19] http://www.mathworks.co.kr/help/toolbox/control/ref/dlqr.html.
[20] B. W. Park, S. H. Jeon, and C. D. Kee, "A closed-form method for the attitude determination using GNSS Doppler measurements," *International Journal of Control, Automation, and Systems*, vol. 9, no. 4, pp. 701-708, December 2011.

Sanghoon Jeon received his B.S. degree from the School of Mechanical and Aerospace Engineering at Seoul National University, Seoul, Korea, in 2004. Currently, He is in Ph.D. course at the School of Mechanical and Aerospace Engineering at Seoul National University. He is the leader of indoor navigation team of GNSS Lab. at Seoul National University. He is interested in GNSS signal processing, attitude determination receiver using GPS, software GNSS receiver.

Chongwon Kim is a Ph.D. student in the School of Mechanical and Aerospace Engineering at Seoul National University, Korea. He received his B.S. and M.S. degrees in Mechanical and Aerospace Engineering from the same university. His research interests include indoor navigations, pseudolites, and GNSS receivers.

Ghangho Kim is a Ph.D. candidate in the School of Mechanical and Aerospace Engineering at Seoul National University, Korea. He received his B.S. and M.S. degrees from Seoul National University. His research interests include astrodynamics and orbit determination using GNSS.

Ojong Kim is a Master student in the School of Mechanical and Aerospace Engineering at Seoul National University, Korea. He received his B.S. degree from Seoul National University. His research interests include APNT and GNSS receiver technology.

Changdon Kee is a Professor in School of Mechanical and Aerospace Engineering at Seoul National University, Korea. He received his B.S. and M.S. degrees from Seoul National University and his Ph.D. degree from Stanford University in 1994. He has been involved in GPS research for more than 20 years, during which time he has made numerous contributions, most notably to the development of the Wide Area Augmentation System (WAAS).